C.2 HMI Science Implementation

The HMI instrument design and observing strategy are based on the highly successful MDI instrument [1] (**Foldout 2.D**), with several important improvements. Like MDI, HMI will observe the full solar disk in the Ni I absorption line at 6768 Å, but with a higher resolution of 1 arc-second. HMI consists of a refracting telescope, a polarization selector, an image stabilization system, a narrow band tunable filter and two 4096x4096 pixel CCD cameras with mechanical shutters. The polarization selector, a pair of rotating waveplates, enables measurement of Stokes I, Q, U and V with high polarimetric efficiency. The tunable filter, a Lyot filter with one tunable element and two tunable Michelson interferometers, has a tuning range of 750 mÅ and a FWHM filter profile of 84 mÅ. Examples of the filter profiles are shown in **Figure C.8**.

C.2.1 HMI Measurement Technique

The basic HMI observables are filtergrams taken at a number of wavelengths and polarizations, all of which are transmitted to the ground. The primary observables, Dopplergrams, longitudinal and vector magnetograms, and continuum intensity images, are constructed from the raw filtergrams by a combination of simple MDI-like algorithms and more complex inversion algorithms. Performing these calculations on the ground is a significant improvement over MDI because more comprehensive instrumental corrections can be made and sophisticated algorithms used in determining the physical solar parameters.

C.2.1.1 Line Choice and Filter Profile

The Ni I absorption line at 6768 Å has been chosen on the basis of our experience with MDI. This line is well characterized and provides continuity with the MDI and GONG helioseismology and magnetic field observations. It has a clean continuum although there are some molecular blends in sunspot umbra. The absence of terrestrial blends allows easy

ground calibration and comparison with ground based data. It has a low level excitation potential[2] of 1.826 eV with little variation in the depth of formation, so its observables apply to approximately the same height in the atmosphere.

The choice of spectral line for magnetic field measurement is driven by conflicting scientific requirements. For magnetic field measurements, a high effective Landé g factor increases the signal, but it also increases the required dynamic range requirements, from ±6.5 km/s (solar rotation, oscillations, convection, and the SDO orbit) to ±12 km/s (g=3 and a 2 kG field). The Ni line provides a compromise with an effective g=1.426, sufficient to reliably measure magnetic fields. ASP observations of an active region in the Ni line (**Figure C.5**) shows that this line performs well for vector field determinations.

The inherent dynamic range of the instrument, ±15 km/s, is set by the spectral range of the filter elements. The effective dynamic range is set by the number and wavelengths of the tuning positions. With five positions spaced by 75 mÅ, the dynamic range is ±6 km/s and each additional tuning position adds ±1.5 km/s. Increasing the spacing much beyond 75
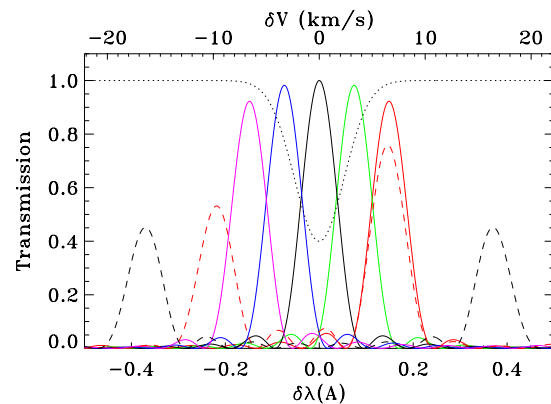

Figure C.8: The solid lines show the HMI filter transmission profiles at 75 mÅ spacing. The black dashed line is the profile used for the continuum filtergram. The red dashed line shows one of the corresponding profiles for MDI. The dotted line shows the Ni I line profile.

mÅ undersamples the line profile. The dynamic range requirement can be reduced by ±1.7 km/s by changing the tuning positions twice per day to follow the orbital Doppler shift. This may introduce discontinuities and increase the calibration accuracy required. Increasing the number of tuning positions reduces the cadence without improving the accuracy per measurement, increasing the noise per unit time.

C.2.1.2 Observing Sequence

The observing sequence design requires careful consideration of cadence, dynamic range, noise level, required polarizations, solar feature temporal evolution, and instrumental effects. Experience with MDI observations shows that deviation from a uniform sequence, such as for synoptic magnetograms or intermittent campaign sequences, cause noise and false peaks in the velocity spectrum. The continuity requirement for helioseismology is to observe more than 95% of the time on all temporal scales with 99.99% data recovery. Therefore, it is essential to use a single continuously running sequence for all HMI observations.

Simultaneous measurements of the Doppler velocity and line-of-sight and vector magnetic field observing requirements impose significant constraints on the sequence. Scanning in wavelength is required for velocity determinations while making multiple polarization measurements quickly is a priority for the magnetic field. An optimal sequence would provide four polarization measurements at five wavelengths in less than 50 seconds. The

available detector technology, however, cannot accomplish this with a single camera. State of the art CCD cameras require about 2.4 seconds to readout a 4096^2 pixel detector, and coupled with the estimated exposure time of 250 msec with reserves pushes a 20 image sequence to a cadence well over 50 seconds.

In order to provide adequate margin in the instrument performance, a two camera design has been adopted. To ensure optimal Doppler performance, one camera is used for the Doppler and line-of-sight magnetic field measurements, the other for the vector field measurements each with a specific polarization sequence. Based on the above, the baseline observing sequence is detailed in **Figure C.9**. The same sequence of wavelength tunings is used for both the vector and line-of-sight measurements. This limits the wear on the tuning motors and ensures that changes in the tuning sequence do not cause artifacts in the line-of-sight measurements.

To measure the full polarization vector at a given wavelength, at least four filtergrams are required. The four polarization measurements are spread out over twice the time required for the line-of-sight measurements. The choice of polarizations and the order in which they are taken drive the observing sequence design for the vector measurements. The sequence shown in **Figure C.9** determines Q in the first half and U in the second half. A ¼ waveplate followed by a ½ waveplate provides the required polarization states while minimizing wear in the mechanisms.

A 45 second cadence is achieved for the Dop-

Time (sec)	0		8		16		24		32		40	45		53		61		69		77		85
λ Tuning	I1		I2		I3		I4		I5		IC	I1		I2		I3		I4		I5		IC
Doppler Seq	L	R	R	L	L	R	R	L	L	R	C	L	R	R	L	L	R	R	L	L	R	C
Vector Seq	1	2	2	1	1	2	2	1	1	2	C	3	4	4	3	3	4	4	3	3	4	C
Polarization	L = I + V = LCP			R = I - V = RCP			1 = I + aQ + bV			2 = I – aQ + bV			3 = I + aU – bV			4 = I – aU - bV						

Figure C.9: Details of the HMI observing sequence: *Time* indicates the beginning of the exposures at a given wavelength. The *wavelength Tuning* positions I1 through I5 are spaced evenly 75 mÅ apart, with I3 centered on the line (see Figure C.8). *Doppler Seq* and *Vector Seq* indicate the order and polarizations settings for the two cameras, with the states L, R, 1, 2, 3, 4 identified by *Polarization*. For a^2=2/3 and b^2=1/3, Q, U and V have identical noise equal to 0.22% in the continuum. IC is a continuum filtergram taken in linear polarization.

pler and longitudinal magnetic field and a 90 second cadence is achieved for the vector magnetic field. Including a continuum tuned image in the sequence results in an image cadence of 4.1 seconds for each camera. The exposures and readouts are interleaved. The images from the two cameras will not be combined during normal analysis.

With a CCD performance of 125,000 electrons/pixel, the exposure time must be known to an accuracy of 5 μsec to meet the science precision requirement of 0.1 G in the line-of-sight magnetic field and 0.1 m/s in the velocity.

Image data will be compressed using a look-up table followed by the lossless Rice-type compression scheme similar to that used for MDI. This algorithm can be implemented very easily in hardware to run at the required rate, and its performance is well understood. The technique has been simulated using very high-resolution images from La Palma, blurring them to make diffraction-limited HMI images, adding appropriate noise and quantization, compressing and decompressing. The compression process adds noise which is statistically well-behaved and is a small fraction of the photon shot noise in magnitude at all intensity levels. A worst case continuum image

of a large sunspot required 6.2 bits/pixel, and quiet Sun areas require only 5.5 bits/pixel, Adding a 10% margin to account for potential differences between the La Palma and HMI images gives a baseline compression efficiency of 6.1 bits/pixel, and bandwidth of 50 Mbits/sec to downlink 4096^2 pixel images with a cadence of 2.05 seconds.

C.2.1.3 Doppler and Line-of-Sight Flux Measurement Technique

Since the computations of the physical observables are performed on the ground, more sophisticated algorithms than those used for MDI can be used. The optimal algorithm for deriving Doppler velocity and line-of-sight flux from the filtergrams is a maximum likelihood fit. The performance of this algorithm for Doppler velocity (**Figure C.10**) is very good out to ±6 km/s with noise of 13 m/s rms at moderate velocities and field strengths. For a line-of-sight field and 100% filling factor, this corresponds to approximately10 G rms noise in flux density. This corresponds to 4 G for a five minute average, which is consistent with the AO requirements. Fields up to 4 kG can be measured with less than 50% increase in the noise.

A simpler and faster algorithm constructs a Doppler velocity signal from each polarization (LCP and RCP). The Doppler velocity measurement is the average of these signals, and the line-of-sight flux density is proportional to the difference. The individual velocities are derived with a simple explicit algorithm, avoiding the computationally expensive maximum likelihood fit. The performance of this algorithm (**Figure C.10**) is essentially as good as the performance of more complex algorithms for moderate field strength, and will be used where fast processing is required such as real time magnetograms.

C.2.1.4 Vector field measurement

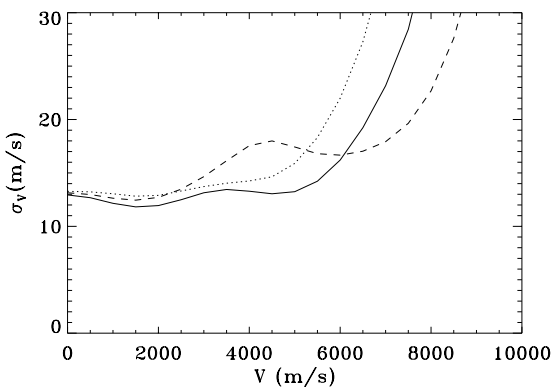A sample strong transverse field signal has been observed with MDI using the proposed

Figure C.10: Doppler velocity noise for the different algorithms. Solid line is for the full maximum likelihood algorithm at B=0 kG, dashed line is for B=2 kG and dotted is for the simple algorithm at B=0 kG.

HMI observing sequence. **Figure C.11** shows a clear Q/I polarization signal. MDI is unable to observe U**.** In the averaged image, linear polarization is visible in the plage, showing that useful signals can be obtained outside of sunspots with a modest amount of temporal averaging.

HMI vector field parameters will be derived with at least two different algorithms. A fast, but not very accurate, algorithm will be applied to the filtergrams as they arrive. A more complex and accurate algorithm will be applied to selected images and to derotated time averages taken over several minutes. The fast algorithm is based on weak-field approximations[3-5] calibration curves[6,7], and provides flux density as well as inclination and azimuth of the magnetic field but not the filling factor or the intrinsic field strength.

The more accurate algorithm fits modeled Stokes I, Q, U, and V signals to the observations using a least-squares minimization method[8] and provides the full magnetic field vector as well as its filling factor. The model profiles are generated with the DIAGONAL algorithm.[9] The minimization uses a singular value decomposition to limit the parameter search to reasonable values and to weight the I, Q, U, and V signals to improve accuracy. This routine is initialized with the results from the simple algorithm supplemented by initial guesses for the filling factor.

The latter algorithm performance has been tested by applying it to simulated data generated using a Milne-Eddington (ME) model, based upon realistic solar values of field strengths, filling factors, and ME thermodynamic parameters. Instrumental details such as the actual filter profiles, photon noise and spacecraft velocity are included in these tests. The differences between the inversion result and the input parameters are taken as a measure of the performance of the proposed instrument. The results are summarized in **Figure C.12** and **Foldout 1.K**. More sophisticated algorithms may be used for the inversions, however the ME results are likely to be representative.

As can be seen from **Figure C.12,** the derived precisions meet the requirements of the active region and sunspot science objectives as well as those for eruptive events at a faster than required cadence. The polarization precision is 0.22% versus 0.3% required; the field precision is 0.8% versus 5% required and the azimuth and inclination errors 0.6° and 1.4°, well within the few degrees required by the AO. Observing network fields is more challenging. The total flux density, for example, has a relative error of 32%. However, for most purposes it is possible to average spatially or temporally. Averaging over 7 observations (10.5 minutes) gives a polarization precision of 0.085%. This translates to a sunspot field precision of 6.5 G or 0.3% in |B|, 0.2° in field
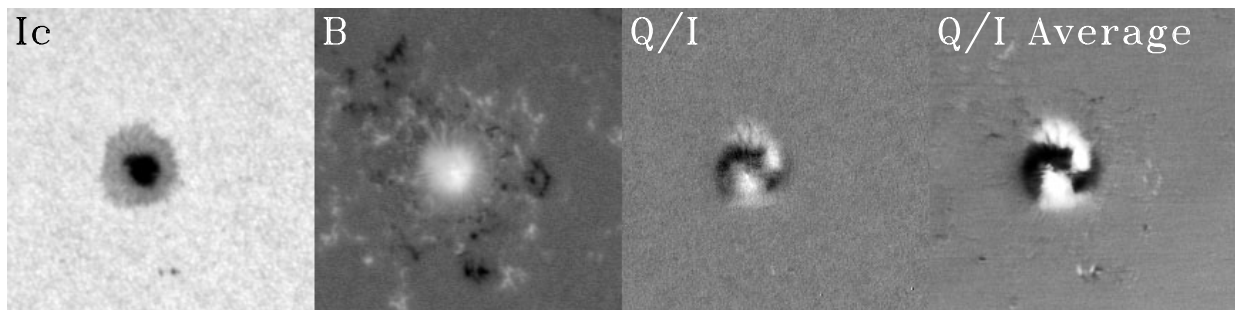

Figure C.11: MDI observations of AR 9516 on 27 June 2001. From left to right: Ic - continuum intensity, B - line-of-sight magnetic field, Q/I - from a single line scan and Q/I Average - a derotated average over 43 observations. The grayscales are not linear in order to accommodate the large dynamic range. The field of view is square of 90Mm on a side with disk center outside the image towards the lower right. The MDI results were taken at a slower cadence than proposed here and without the third tunable element, making them noisier than the expected HMI results.
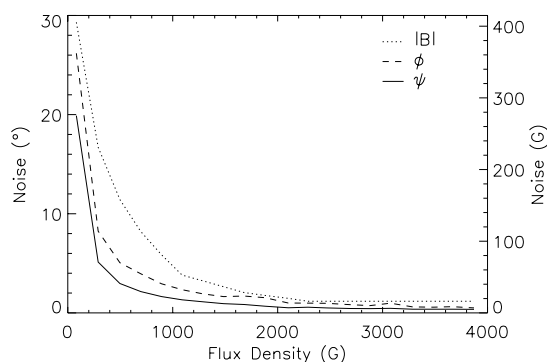
Figure C.12: Azimuth, inclination and field strength at 68% confidence intervals derived from the inversion algorithm. Precisions are for single unaveraged pixels.

inclination, 10 G or 0.9% in the transverse field component, and 0.5º in the transverse field direction. For quiet Sun fields, the precision is 6.1 G or 12% in longitudinal flux density, 17 G or 32% in transverse flux density, 13 G or 12% is total flux density, 6.7º in inclination, and 8.9º in azimuth. Similar improvements can be obtained by spatial averaging.

C.2.1.5 Other Observables

In addition to Doppler shift and field measurements, continuum intensity images will be produced from the continuum filtergram with a small correction for the line contribution. **Figure C.8** shows that the addition of the third tunable element greatly reduces sidelobes, which cause crosstalk of velocity and magnetic field into the continuum images. Line depth (modulation) images and various calibration measurements will be produced as needed.

C.2.1.6 Observable Calibration

Several corrections and calibrations will be applied to the raw filtergrams in order to generate observables with required accuracy and precision. The high radiation levels in geosynchronous orbit generate corrupted pixels in the images. These artifacts are easily identified by statistical means and corrected by interpolating adjacent pixels or marked as missing. The filtergrams will be corrected for the

bias and actual exposure time and flat fielded. This allows the filtergrams to be interpolated to compensate for relative offsets introduced by the polarization and wavelength selectors and by solar rotation.

The ±3.5 km/s variation in the line of sight velocity due to the SDO orbit then provides a means of velocity calibration over a large fraction of the tuning range.

Wavelength and polarization selection are accomplished by rotating elements that may cause small image displacements. In order to allow for spatially interpolating the data, the offsets should ideally be less than 0.1 pixels. However, since the optical PSF is critically sampled, larger offsets can be compensated for, especially if they are highly repeatable. This also means that one should avoid combining images from the two cameras. Similar problems are introduced by the different alignment of the cameras and any differences in the PSF or flat field.

Since the images are taken at slightly different times some of the filtergrams, such as the pairs used for measuring polarization, will be interpolated in time to compensate for the change in the line Doppler shift. Simulations show that the interpolations such as those needed for this can be made without adding significantly to the photon noise.

The measured Stokes parameters are derived from linear combinations of the observations taken in the four polarization states. These need to be corrected for the instrumental effects of the telescope and polarizers to obtain the true (input) Stokes vector. This is performed by multiplication of the observed vector by an instrument response matrix obtained by measuring the response of the instrument to known polarization states.

C.2.2 HMI Instrument Description

The HMI instrument is shown in **Foldout 2.A**. Sunlight travels through the instrument from upper right to lower middle in the schematic. The front window is a multilayer metal-dielectric filter with a 50 Å bandpass centered at 6768 Å that reflects most of the incident sunlight. The window is followed by the 14 cm diameter refracting telescope.

Two focus/calibration mechanisms, two polarization selection mechanisms and the image stabilization system tip-tilt mirror are located between the telescope and the polarizing beamsplitter feeding the tunable filter. The filter section consists of the following elements, which are contained in a precisely temperature-controlled enclosure.

- A telecentric lens.
- An 8 Å bandpass dielectric blocking filter.
- A Lyot filter with a single tunable element.
- Two tunable wide-field polarizing Michelson interferometers.
- Reimaging optics.

Following the oven is a beam splitter, which feeds two identical shutters and CCD camera assemblies. There are two mechanisms external to the optics package: a front door, which protects the front window before launch, and an alignment mechanism that adjusts the optics package pointing.

C.2.2.1 Optics

The primary imaging optics are a refracting telescope similar to the MDI design except that the primary lens has a 14 cm aperture compared with 12.5 cm on MDI. This gives a critically sampled diffraction limited image with 1.0 arc-second resolution. The primary and secondary lenses are connected with a low coefficient of expansion metering tube to maintain focus.

The total optical path length is 225 cm with an effective focal length of 485 cm and a focal ratio at the final image of 34.6. The raytrace

(**Foldout 2.C**) shows the imaging mode paths in black and the calibration mode paths in red.

The HMI calibration configuration and focus adjustment method is identical to the MDI instrument. Two calibration/focus wheels each contain optical flats of varying thickness in four positions to provide focus adjustment in 16 steps. Besides allowing best focus to be set on orbit, this capability also provides a highly repeatable means for measuring the instrument focus and assessing image quality through phase diversity analysis.

In calibration mode, a lens in the fifth position of each wheel images the entrance pupil onto the focal plane to provide uniformly integrated sunlight. This provides an excellent velocity calibration source for the instrument. Calibration mode images are used to provide Doppler calibrations, monitor the instrument transmission and assess variations in the detector flatfield.

The polarization selectors rotate optical retarders to convert the desired incoming polarization into vertically polarized (s-component) light. The light is folded by the ISS mirror and then split by a polarizing beamsplitter to send the s-component light to the filters while passing the orthogonal light onto the limb sensor. The limb sensors receive the full 50 Å bandwidth, while light for the rest of the instrument continues through the 8 Å bandpass blocking filter located just inside the oven.

A telecentric lens at the entrance of the filter oven produces a collimated beam for the subsequent filters. This ensures that the angular distribution of light passing through the filters is identical for each image point, resulting in a uniform wavelength selection over the detector.

At the exit of the oven, a pair of lenses reimages the primary focus onto the detectors. A beamsplitter evenly divides the light between the two camera paths with a pair of folding mirrors used to provide convenient placement

of the vector magnetic field camera. The shutters are placed near the pupil image.

The glass-vacuum interfaces are anti-reflection coated for high efficiency at 6768 Å. The polarization selection and tuning waveplates will be manufactured to tight wedge and distortion tolerances in order to minimize displacements due to their rotation. The MDI Michelson tuning waveplates met these stringent conditions.

C.2.2.2 Filters

The heart of the HMI instrument is the filter system consisting of the front window, a fixed blocker filter, a Lyot filter with a single tunable element, and two tunable Michelson interferometers. Doppler shift measurements of solar oscillations require a filter system with a very stable and reproducible passband. Both the Lyot filter and the Michelson have temperature compensating designs, and all the filters, except the front window, are mounted in an oven stable to ±0.1 ºC. The filter system enables narrow-band filtergrams to be made across the Ni I 6768 Å line by co-tuning one Lyot tunable element and the Michelson interferometers. The combined filter bandpass is 84 mÅ with a tunable range of 750 mÅ.

The front window is a 50 Å bandpass filter. It is similar to the MDI design that consists of bonded glass optical flats with a multilayer dielectric coating sandwiched in between. The design will be reviewed to ensure that appropriate radiation hardened materials and processes are used in fabrication.

The blocking filter is a three-period all-dielectric interference filter with a bandpass of 8 Å. The MDI blocker transmission profile has a ripple of about 1%, which averages out to less than 0.1% over the beam. The temperature sensitivity of the MDI blocker is 0.2 Å/ºC, and current ion-assisted coating technology will provide an order of magnitude lower temperature sensitivity.
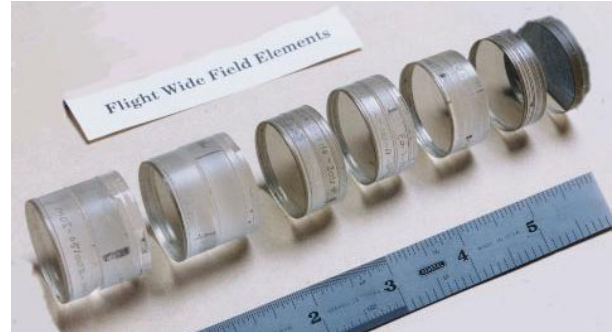

Figure C.13: The MDI Lyot elements and blocking filter.

The wide-field, temperature-compensated Lyot filter (**Figure C.13**) will use the same basic design as the MDI filter with the addition of a fifth tuned element. By pairing KDP or ADP elements with the calcite elements, the temperature sensitivity in the calcite is compensated by an opposite change in the KDP/ADP. The MDI Lyot has a measured temperature sensitivity of less than 8 mÅ/ºC. The five-element Lyot filter has a 1:2:4:8:16 design, and a bandwidth of 380 mÅ. The Lyot components are held in optical contact by optical grease, and are keyed to hold the elements in proper relative alignment.

Figure C.14: The MDI flight Michelsons are shown with the 'Stonehenge' copper spacers to reduce stress. Kapton tape maintains cleanliness prior to installation.

The final filters are a pair of wide-field, tunable solid Michelson interferometers (**Figure C.14**) with a clear aperture of 45 mm and free spectral ranges of 190 mÅ and 380 mÅ (95 mÅ and 190 mÅ bandpasses respectively). The design is identical to that used in MDI and incorporates a polarizing beamsplitter with a vacuum leg and a solid glass leg. The

vacuum leg is maintained with temperature compensating copper standoffs. Tuning is accomplished by rotating half-wave retarders mounted between the interferometers.

The MDI Michelsons have gradients in central wavelength of tens of mÅ across their faces; after calibration these gradients have not significantly affected MDI measurements. For HMI, we expect lower gradients as a result of our experience in fabricating the MDI and GONG Michelsons.
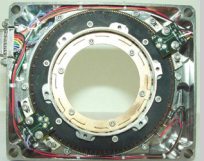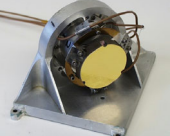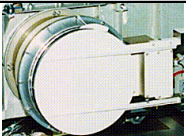
C.2.2.3 HMI Mechanisms

The HMI instrument contains 11 mechanisms of 5 different types, each of which has extensive heritage on the MDI, TRACE, SXI-N, and Solar-B/FPP programs. On-orbit performance with MDI gives us confidence that we will achieve the high performance required of the two most frequently used mechanism types – the camera shutters and the hollow-core motors used for polarization selection and filter tuning. **Figure C.15** shows the positions of each of these mechanisms in the HMI optics package.

The shutters are identical to those on MDI and SXI, and provide exposure measurement with an accuracy of 4 μsec. Because every HMI image will be downlinked, variations more than an order of magnitude larger than those seen on MDI after 60 million operations will cause no detrimental effects.

The hollow-core motors are copies of the units being used in the SECCHI coronagraphs, which are improved versions of those that have made more than 60 million moves on MDI. The repeatability required of these units has been demonstrated on MDI. The HMI

Mechanism (# required)	Performance		Illustration
Shutter (2) MDI and SXI heritage stepper motor with 94 mm blade.	Maximum Beam Diameter: Exposure Range: Repeatability / Accuracy Required Life:	15.2 mm 40 msec to 90 sec ± 10 μs / ± 0.5 ms 80 M operations	
Polarization Selector (2) and Filter Tuning (3) Motors MDI and SECCHI heritage, 50 mm clear-aperture hollow core motor with 2.5° step size.	Maximum Beam Diameter: Single Operation Time: Repeatability /Accuracy: Required Life:	39.5 mm < 800 msec / 60° ±30 arcsec / ±2 arcmin 160 M operations	
Calibration-Focus Wheel (2) MDI and SXI heritage, 90 mm brushless DC motor with five 30 mm apertures.	Maximum Beam Diameter: Single Operation Time: Required Life:	26.0 mm < 800 msec (1 filter step) 20,000 operations	
Image Stabilization System MDI and Trace heritage ISS design.	Stability: Range: Frequency Range: Required Life:	0.1 arcsec / 30 sec ± 10 arcsecs X & Y 0-200 Hz 10 years	
Aperture Door MDI heritage design. Includes redundant drive motors.	Aperture Diameter: Required Life:	160 mm 1000 Operations	
Alignment Mechanism MDI heritage two-leg adjustment system.	Range / Resolution: Required Life:	±720 arcsec / ±5 arcsec 1000 operations	
Table C.1 - HMI Mechanisms			

focus/calibration wheels are functional copies of SXI-N units with five rather than six elements. They will primarily be used for calibration a few times per day.

The aperture door and pointing alignment mechanisms are based on MDI designs. The HMI alignment mechanism can adjust the optics package pointing over approximately 13 arc-minutes, and will be used to center the solar image on the CCD. The duty cycle will be similar to MDI where the front door has been operated only three times on orbit and the alignment mechanism is typically used every eight weeks.

Table C1 details the design and heritage of each of the HMI mechanisms. The shutter, focus/calibration wheel, and wavelength selector mechanisms use brushless DC motors that have high torque margins and robust bearing designs. The mechanisms are constructed for an operational lifetime at the image capture cadence of four seconds for 10 years. Preliminary analysis indicates that angular momentum compensation is not required.

Because of their frequent use, life testing is planned for the hollow core motors and shutters. The lifetests will be performed in a vacuum chamber with the mechanisms at their nominal operating temperatures (20 ºC for the polarization selector and shutters and 35 ºC for the Michelson tuning motors), after having been subjected to vibration testing. The lifetest goal is to achieve the equivalent of 10 years of mechanism moves. The basic design, performance, and life test methodology is similar to the MDI mechanism lifetest.[10]

C.2.2.4   Image Stabilization System

The HMI Image Stabilization System (ISS) is a closed loop system with a tip-tilt mirror to remove jitter measured at a primary image within HMI. This system is based on the MDI ISS limb sensor, mirror and servo loop.

Jitter of photospheric features results in intensity fluctuations that translate into velocity

and magnetic field errors. Even though image co-alignment can be performed on the ground, interpolation of images over more than a few tenths of a pixel causes loss of information. The HMI stabilization requirement is set at 0.10 arc-second (3-sigma) in each axis.

The ISS uses the image of the solar limb projected onto four orthogonal detectors at the guiding image focal plane. Each detector consists of a redundant photodiode pair. The electronic limb sensor photodiode preamplifier has two gains, test mode and Sun mode, and selectable prime or redundant photodiodes. This is identical to the MDI design, with only an obsolete op-amp being replaced for HMI.

The mirror uses a 3-point piezoelectric transducer (PZT) actuator to remove errors in the observed limb position. The tip-tilt mirror uses the same low voltage PZT's and drive circuitry as MDI. This mirror design has a first resonance (>500 Hz) much higher than the structural mode of the HMI optics package, enabling a simple analog control system.

The range of the tilt mirror is elongated, approximately ±12 by ±18 arc-second. This can be increased significantly by using longer PZT's of the same type, if judged necessary during Phase A evaluation of the spacecraft pointing.

The servo gains and other parameters are fully adjustable by computer commands. In particular, offsets can be added to the X and Y axis error signals to change the nominal pointing while maintaining lock. Individual PZT actuator offsets can be specified to fix the nominal position of the mirror anywhere in its range during open loop operation or during special calibrations.

The error and mirror signals are continually sampled, and down-linked to monitor jitter and drift. For special calibrations, these signals can be sampled at a higher rate.

C.2.2.5   CCD and Camera Design

The HMI instrument contains two identical CCD detectors, with a 4096×4096 pixel format. These CCDs are a Marconi Applied Technologies (formerly EEV) design that is an extension of the 2048×4096 pixel devices being used on the Solar-B/FPP. The CCDs are front-illuminated with 12-μm pixels and operated non-inverted to ensure a full well capacity of 150k to 200k electrons with an anticipated readout noise of less than 12 electrons. They will be cooled to below –65 ºC resulting in a 1 nA/cm² dark current (0.2 e⁻/pixel-sec). They feature low-voltage clocking of the serial output register to minimize power dissipation in the clock driver electronics. Marconi has a long history of manufacturing excellent CCD devices for space flight applications, including the sensors for Solar-B/FPP and the SECCHI instruments.

In order to achieve readout in less than 3 seconds, they have a readout rate of 2 Mpixels/s through each of four quadrant readout ports. Multiple ASIC and surface-mount electronics packaging technologies minimize the size, mass, and power requirements of the cameras.

A single HMI camera electronics unit controls both CCDs. The HMI camera electronics unit is comprised of:

1. Two CCD Driver Cards, one dedicated to each CCD detector.
2. A camera Housekeeping and Telemetry card with master crystal oscillator clock supply for the CCD Driver Cards.
3. A DC-DC Power Converter mounted on the base of the electronics box.
4. A backplane interface for inter-connection of the daughter PCBs.

Each CCD is clocked from its own dedicated sequencer and clock drivers, and is read out through four correlated double samplers and 14-bit analog to digital converters operating in parallel. The electronics exploits the same basic waveform generator and clock driver circuit topologies used for the SECCHI cameras. This design is implemented in an ASIC similar to the radiation tolerant chip developed for the SECCHI program at Rutherford Appleton Laboratory (RAL), but re-optimized for the 2 Mpixels/s readout rate and signal gain of the HMI CCD. The video output gain and DC offset level are programmable.

Each CCD Driver Card communicates with the instrument computer via an IEEE1355-SpaceWire link, enabling camera programming, camera command, gathering of housekeeping data, and the transmission of digitized data at up to 200Mbits/s. Exposure timing is controlled directly from the HMI instrument computer.

The camera controller contains a DC-DC power converter driven from the 28V spacecraft primary power, while the decontamination heater power for the CCD heads is routed from the HMI power distribution system. The controller's internal temperature and power supply voltages are monitored by the camera electronics while the CCD temperatures are monitored by the HMI computer.

C.2.2.6   Structure

The HMI Optics Package (**Foldout 2.B**) structure is a bonded honeycomb design similar to that used for the much larger Solar-B FPP, the structural model of which recently completed qualification vibration tests. The HMI structure is a six-sided box with a removable cover made up of panels consisting of vented aluminum honeycomb core with aluminum face sheets (**Figure C.15**). The base panel will be 25 mm thick with 0.5 mm face sheets, and functions as an optical bench for mounting the optical components except the CCD detector assemblies. All other panels are 6 mm thick with 0.25 mm face sheets.

Construction techniques are the same as those used on the FPP. Panels are joined by bonded L-section sheet connectors and machined sections where necessary. All panel penetrations
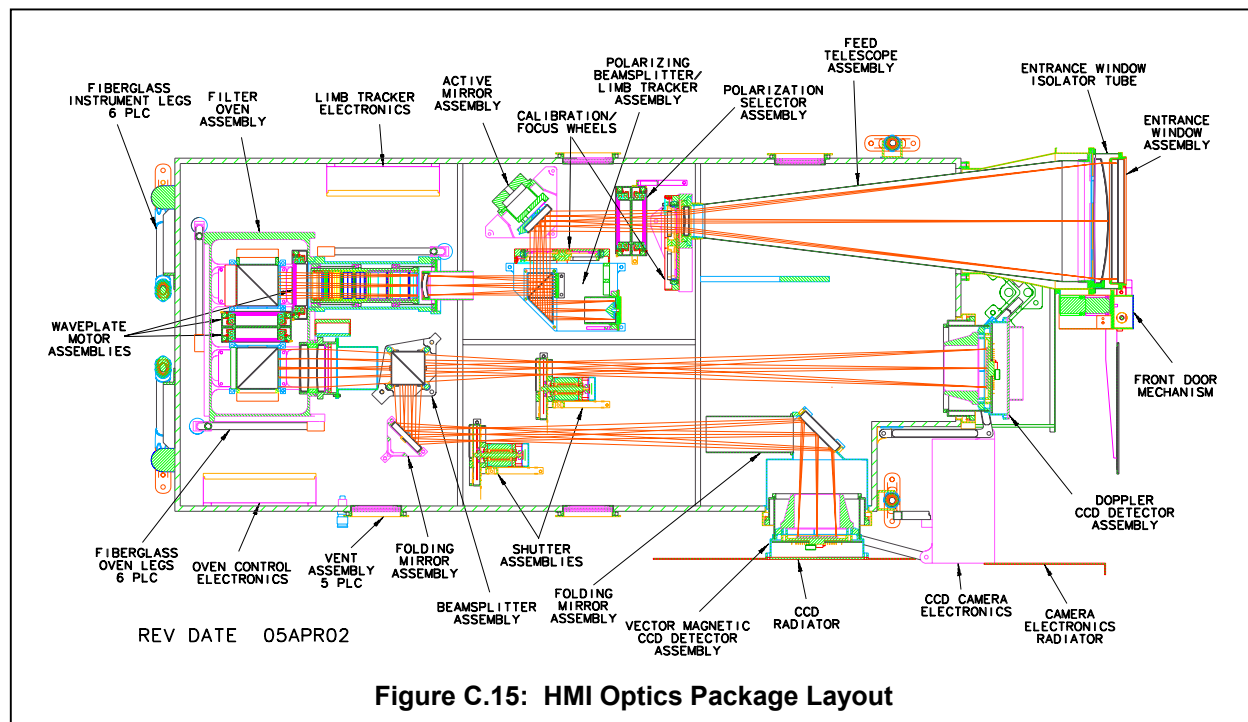
Figure C.15: HMI Optics Package Layout

are sealed with machined closeouts, and have vent paths to the exterior for cleanliness. Component subassemblies are mounted to machined brackets bonded to the optical bench; flanged through-panel inserts capture the brackets to avoid tensile loads on the bonds and crush loads on the core.

The Optics Package mounts to the spacecraft with a 6-link kinematic mounting system incorporating a pointing mechanism similar to MDI. The pointing legs and two forward/side vertical legs are located similar to MDI; the other two are reoriented to share the thrust load between both of them instead of the single thrust leg design used on MDI. The leg construction is identical to MDI: fiberglass tubes for thermal isolation, with bonded end fittings and rod ends to accommodate pointing motion.

A finite element model has not yet been performed, but based on experience with MDI and FPP, no difficulty is anticipated in achieving adequate stiffness and strength. Both the MDI and FPP optics packages have first mode resonant frequencies of about 85 Hz. Mass properties are summarized in **Table C4**. They

are based on measured MDI flight hardware, the detailed HMI solid model, and on similar FPP components.

C.2.2.7 Thermal Control

Evaluating the impact of the MDI thermal performance on the science observations provides the key to achieving the demanding thermal requirements for HMI. The MDI design experience and performance data, combined with experience on the SXI-N, Solar-B and SECCHI programs and expertise in integrated state-of-the-art analytical tools, is a valuable asset to the HMI thermal engineering team.

The HMI instrument is thermally isolated from the spacecraft. Thermal stability is achieved using passive radiator surfaces and controlled heaters. The optics package is mounted on fiberglass legs to thermally isolate it from the spacecraft, and a zone heater maintains the optics package to ±0.5 ºC. The CCD detectors are maintained at less than –65 ºC by passive radiators.

The camera electronics box is partially decoupled thermally from the optics package

Thermal Design	Performance	
Aperture Door MDI design: Coatings tailored to maintain door near ambient temperature whether open or closed.	Operating / Survival Temps: Door Open Angle:	0 to 40 °C / -20 to 65 °C 180°
Front Window Improved MDI design: Heaters around perimeter minimize recovery time after eclipse.	Operating / Survival Temps: Max Oper Radial Gradient: Max Recovery After Eclipse:	0 to 50 °C / -20 to 65 °C 2 °C center to edge 1 Hour
Filter Oven MDI design: Closed loop thermal control of isolated oven maintains temperature of critical components.	Operating Temperature: Max Temperature Drift:	35 ± 0.1°C 0.01 °C/hour
Optics Package Thermal Control System SXI design. Software-controlled zone heater to minimize gradients and transients.	Operating / Survival Temps: Setpoint Control: Max Gradient:	15 to 25 °C / 0° to 45 °C ± 0.5 °C 4 °C
CCD Detectors FPP design. CCDs thermally decoupled from housing & passively cooled via dedicated radiators.	Oper / Survival Temps: -100 to –30 °C / -120 to 45 °C Decontamination Temp: 20 to 40 °C	
Table C.2 - HMI Thermal Requirements		

and passively cooled via its own dedicated radiator. The main (and remote) electronics box is passively cooled via a dedicated radiator.

A precisely controlled oven houses all of the narrow band filters. A closed loop heater similar to the MDI design maintains the oven to ± 0.1 °C of a set point with a maximum drift of 0.01 °C/hr. The oven is mounted on a set of fiberglass legs thermally isolating it from the optics package. The operating temperature of the oven is selectable.

The front window is thermally isolated from the rest of the optics package, and the absorptivity/emissivity ratio is tailored to operate near 20 °C. Special attention must be paid to the front window thermal control during eclipses because radial gradients in the window change the instrument focus and birefringence. **Figure C.16** shows the response of the front window to a one-hour eclipse. The first case has no thermal control and indicates a recovery time greater than three hours. The second case has 9 W of heat applied at the edge of the window during the eclipse. Although the radial temperature gradients increase due to the heat input, the recovery time is less than an hour. Additional thermal modeling will be developed during Phase A to achieve an optimal design.

Detailed board-level and box level thermal analysis is performed to verify that adequate heat sinking is provided. Heaters will either be Kapton film, non-inductive types or power resistors where concentrated heat is required.

C.2.2.8 Electronics

The HMI electronics are shown in the functional block diagram in **Foldout 2.E**, and can be divided into 6 subsystems: control computer; camera electronics; camera interface/buffer; ISS, mechanism control electronics; and power electronics. The camera electronics (C.2.2.5) and ISS (C.2.2.4) were previously discussed.
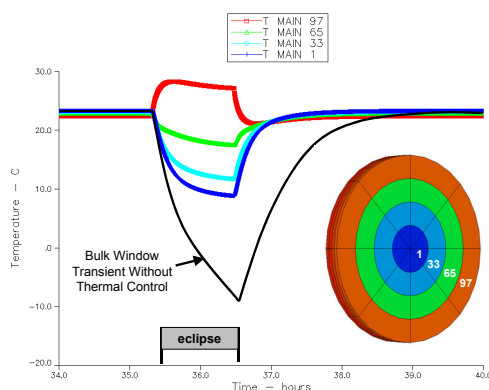

Figure C.16: Front window temperature response to a 1-hour eclipse. The black curve is with no additional thermal control. The colored curves show the temperature response from edge (red) to center (blue) with 9W heat input at the window perimeter during the eclipse.

The control computer subsystem consists of the RAD750 control computer, spacecraft interface, housekeeping data acquisition system, and a PCI bridge that uses a standard compact PCI bus. The BAe RAD750 processor is being used on the SECCHI program, and is the next generation from the RAD 6000 processor with which LMSAL has extensive experience on the SXI-N and Solar-B/FPP programs. The RAD750 control computer runs on a single 3.3-V power source and is packaged on a 3U format card with 128 MB of SDRAM, 256KB of Start-Up ROM (SUROM), and EEPROM loaded with the flight software. The HMI power-on initiates the control computer boot loader that transfers the flight software from EEPROM and starts the control software. The EEPROM data can be modified by ground command if necessary after launch.

A Summit type remote terminal controller connects to the spacecraft redundant Mil 1553 control and low rate data bus. A LVDS bus interface is provided for the 55 Mbps science data stream. The temperature, voltage, current, and other data needed to monitor the HMI instrument are acquired by the housekeeping data system and transferred to the control computer where they are formatted into CCSDS housekeeping packets. The PCI bridge provides a control interface from the PCI bus to the camera interface and buffer, mechanism control electronics, and image stabilization system.

The camera interface and buffer subsystem acquires science data from the two HMI camera systems, optionally compresses the data, and prepares it for transfer to the spacecraft LVDS interface. Two fully independent camera interface and buffer subsystems can simultaneously acquire data from their associated cameras. Each has buffer memory for two images, so that an image can be passed to the data compressor while another image is being acquired from the camera.

The single data compressor acquires data sequentially from the two camera interfaces as directed by the control computer. The data is then formatted into standard CCSDS packets and passed on to the spacecraft interface.

The mechanism control electronics are minor modifications of the control electronics developed for the Solar-B/FPP and SECCHI programs. There will be three mechanism controller boards, which also provide control for the operational heaters.

The main power subsystem, located in the electronics package, provides conditioned power for the digital electronics, mechanisms and the filter oven heater. The HMI power converters contain the inrush current limiting and EMI filters needed to meet the spacecraft EMI/EMC specifications. The power systems have heritage from the TRACE, SXI-N, and Solar-B/FPP programs and are designed around radiation hardened modules such as those from Interpoint or Lambda.

C.2.2.9 Software

The flight software uses the VxWorks operating system and will be written in C and C++ using the Tornado development environment. Extensive experience exists within LMSAL using the VxWorks operating system on programs including HIRDLS, SXI-N, and Solar-B/FPP. The flight software will interface with the spacecraft over a 1553 bus for commands and housekeeping.

Images are produced under control of stored observing sequences selected by ground command. Exposure timing is locked to an internal reference updated by the spacecraft clock signals. The flight software controls the shutters, polarization selectors, tuning motors, and calibration-focus wheels as part of observing sequences. CCD camera data are moved through the data system independent of the processor bus. Software only controls the transfer of the images, and does not perform any on-board image processing.

The ISS and filter oven heater are closed loop systems that run independently of the flight software with control parameters updated by ground command. Other heaters are controlled by the flight software to maintain temperatures set by ground command A limited amount of on-board fault management is provided to gracefully accommodate certain malfunctions or failures.

The specified control functions will use less than 50% of the CPU capability. Memory will be sized such that less than 50% is used at launch. Capability to upload a new code image and/or to patch the flight code exists in the SUROM. An incremental code development approach will provide additional capabilities to support hardware elements as they are available for test and integration.

C.2.2.10 Radiation Protection

The RAD750 system is latchup immune, rated at 2M rad total dose, and has an error rate of $1x10^{-10}$ errors/bit day SEU. The other electronics are similar technologies to those used on previous missions. They include rad-hard analog components, HSC-family digital electronics, FPGAs and ASICs. The power distribution system will be implemented with rad-hard converters (100K rad, no latchup or SEU, no opto-couplers). All power switching components are rad-hard MOSFETs as screened and used on previous programs.

Radiation analysis is performed on each component and, where appropriate, radiation testing of the actual component type is performed to ensure adequate radiation performance and/or shielding requirements. The electronics are designed to provide adequate margins after accounting for radiation degradation and the enclosures provide a minimum of 5 mm of Al for radiation shielding. The HMI CCDs are designed to operate in the geosynchronous orbital radiation environment. The CCD mounting design has 10 mm of Al shielding.

C.2.2.11 Resources and Accommodations

The required spacecraft resources for the HMI instrument are shown in **Table C.3**. A 20% reserve has been allocated both the mass and power. The science telemetry is 50 Mbps with a 10% reserve of 5 Mpbs. The housekeeping telemetry is 10 kbps. Commanding is expected to be one to two uploads per week except during the initial commissioning activities. When in operation, HMI will not have significant power variations. Increased heater power is required during eclipses. A preliminary power

Table C.3 HMI Resource Requirements	Optics Package	Camera Electronics	Electronics Package	Cable Harness	Reserves	Total
Mass (kg)	25	3	15	3	9	55
Length (cm)	118	19	32	200	-	-
Width (cm)	53	15	28	-	-	-
Height (cm)	24	7.5	21	-	-	-
Electronics Power (W)	-	15	40	-	11	66
Ops Heater Power (W)	5	0	0	-	1	6
Temperatures (ºC)						
Maximum Survival	45	50	50	-	-	-
Maximum Operational	25	30	30	-	-	-
Minimum Operational	15	0	0	-	-	-
Minimum Survival	0	-20	-20	-	-	-

The camera electronics volume is included in the Optics Package envelope dimensions

profile is shown in **Table C.4**.

The optics package is mounted onto a panel of the instrument module via the support legs. The HMI electronics box is mounted to the spacecraft separately from the optics package. Locating the HMI electronics box inside the spacecraft could save some mass required for radiation shielding. The optimal location and

Table C.4 HMI Mode	Time	Nominal Power (W)	Reserve (W)	Max Power (W)
Power Off		0	0	0
Survival Heat On	~12 hrs	45	9	54
Instrument On	Normal	60	12	72
Eclipse	< 60 min	69	14	83
Decontam. On	~4 hrs	70	14	84

mounting scheme for the optics and electronics packages will be developed with the spacecraft builder during Phase A.

The HMI instrument has no special environmental requirements (beyond GEVS) other than the spacecraft must meet cleanliness requirements. HMI will require nearly continuous purging with dry nitrogen until shortly before launch.

C.2.2.12 Calibration

The success of the HMI investigation depends on an excellent calibration of the system. The HMI calibration requirements are summarized in **Table C.5** and are based on our MDI experience. HMI will be thoroughly calibrated before delivery, using techniques developed and proven during the MDI and Solar-B/FPP programs. The LMSAL Sun lab has facilities to calibrate components, subsystems and the complete instrument, using tunable laser, con-

tinuum lamp and sunlight sources, in vacuum when necessary. Most of the calibrations will also be performed on-orbit throughout the mission using the built-in capabilities for tuning, focusing, offset pointing and imaging.

For Doppler measurements, the key measurements are the central wavelengths of the Michelson and Lyot filter profiles. All GONG and MDI Michelsons have gradients in central wavelength across the face of the filter, and all have drifted slowly in wavelength over time. The gradients can be measured accurately both on the ground and in orbit, and drifts can be calibrated accurately in orbit using integrated sunlight in calibration mode as a reference. For normal observing, the two Michelsons and tunable Lyot element are tuned together in wavelength. However, by tuning them independently in a "detune" calibration sequence, the central wavelength of each filter can be measured separately with respect to

Parameter	Accuracy	Purpose	Method
Michelsons Central Wavelength	±1 mA for narrow, ±2 mA for wide Michelson.	Accurate zero-point for velocity across the FOV, system transmission profile	Tunable laser (G), integrated sunlight in calibration mode (G, O).
Lyot Tunable Element Central Wavelength	±4 mA at each point in the FOV	Accurate zero-point for velocity across the FOV, system transmission profile	Tunable laser (G), integrated sunlight in calibration mode (G, O).
Michelson & Lyot Transmission Profile	±2% of peak transmission	Calibration of velocity & magnetic field algorithms	Tunable laser, integrated sunlight with spectrometer (G); computation using measured central wavelengths (O).
Blocking Filter Transmission Profile	transmission	Velocity zero-point , removal of "velocity fringes"	Spectrophotometer measurements (G)
Image Scale	0.01%, or 0.25 pixel limb location	Accurate mode frequencies, especially from ridge fitting; limb figure.	Targets (G, lower accuracy), solar diameter measurement (O).
Distortion of imaging system	0.2 pixel goal, with respect to uniform grid	Accurate mode frequencies; limb figure; correlation tracking.	Grid images (G, lower accuracy), S/C offset pointing, eclipses (O).
Distortion due to waveplate rotation	0.05 pixel with respect to reference position	Alignment for velocity & magnetic measurements; correlation tracking.	Local coalignment of continuum images (G & O)
Optical Point Spread Function	5% of peak	Accurate mode frequencies, especially from ridge fitting; limb figure.	Phase diversity inversion using images at various focus positions (G & O)
CCD Point Spread Function	5% of peak	Accurate mode frequencies, especially from ridge fitting; limb figure.	Direct measurement of ensemble of line spread functions (G)
CCD Flat Field	0.5%	Image correction for velocity, magnetic & continuum, limb figure.	Offsets by PZT's, legs, and occasional S/C offset pointing (G & O)
CCD Dark Images, Gain & System Noise	0.1% for darks, 5% for gain & noise	Image correction, noise estimates for observables.	Dark images & light transfer curve measurements (G & 0)
Overall Optical Efficiency	0.5%	Long-term instrument monitoring.	Synoptic calibration mode images in continuum (O)
Polarization, Mueller Matrix	~ 1%	Accuracy of longitudinal & vector magnetic measurements	Measurements with accurately varied polarization using Solar-B GCU (G).
Polarization Response Changes	1%	Monitor changes from Mueller matrix measured on ground.	Consistency between ground calibration & observations (O).
G – Ground Calibration; O – On-Orbit Calibration			
Table C.5 – HMI Calibration Plan			

integrated sunlight, at each pixel on the Sun. These data will be used to calibrate the velocity and magnetic measurements with an accurate spectral response for each pixel.

The imaging system calibrations are simple in principle but are pushed to very high levels of accuracy by the requirements of helioseismology. These are based on analysis of MDI data, such as the flat field, waveplate distortion and PSF measurements. The CCD calibrations have been routinely done on MDI and Solar-B FPP.

The observations needed to calibrate the various observables will be taken at different intervals depending on the time scale of the variations. The list of calibration measurements include solar and objective image (detuned) filtergrams used to determine Michelson gradients and flat fields, spatially offset images[11] to determine flat fields, dark exposures, sequences to calibrate the instrumental gain, sequences to determine the offsets introduced by the polarization and tuning mechanisms and sequences to determine the instrumental polarization. Most of these calibrations have been developed for MDI or will be similar to those for other vector magnetographs.

Following the strategy employed for the spectropolarimeter on the Solar-B FPP, a polarization calibration unit will not be included in HMI. The response matrix will be determined through pre-flight calibration using the Ground Calibration Unit (GCU) developed at HAO for the Solar-B spectropolarimeter. The GCU introduces beams whose polarization is varied in precisely known ways into the instrument. Analysis of the HMI data yields the polarimeter response matrix (essentially the Mueller matrix). Redundancy in the procedure allows determination of all relevant parameters of the input beam, GCU and HMI simultaneously. Experience has indicated that the instrument response matrix is very stable with time, and will be monitored in flight by comparing HMI observations against those obtained from the ASP and the polarimeter on Solar-B.

C.2.2.13 Build, Assembly, and Test flow

The assembly and testing of optical subsystems will be performed with a series of test and alignment fixtures. The goal is to have the flight optics and filter systems assembled as

Figure C.17: HMI build, assembly and test flow
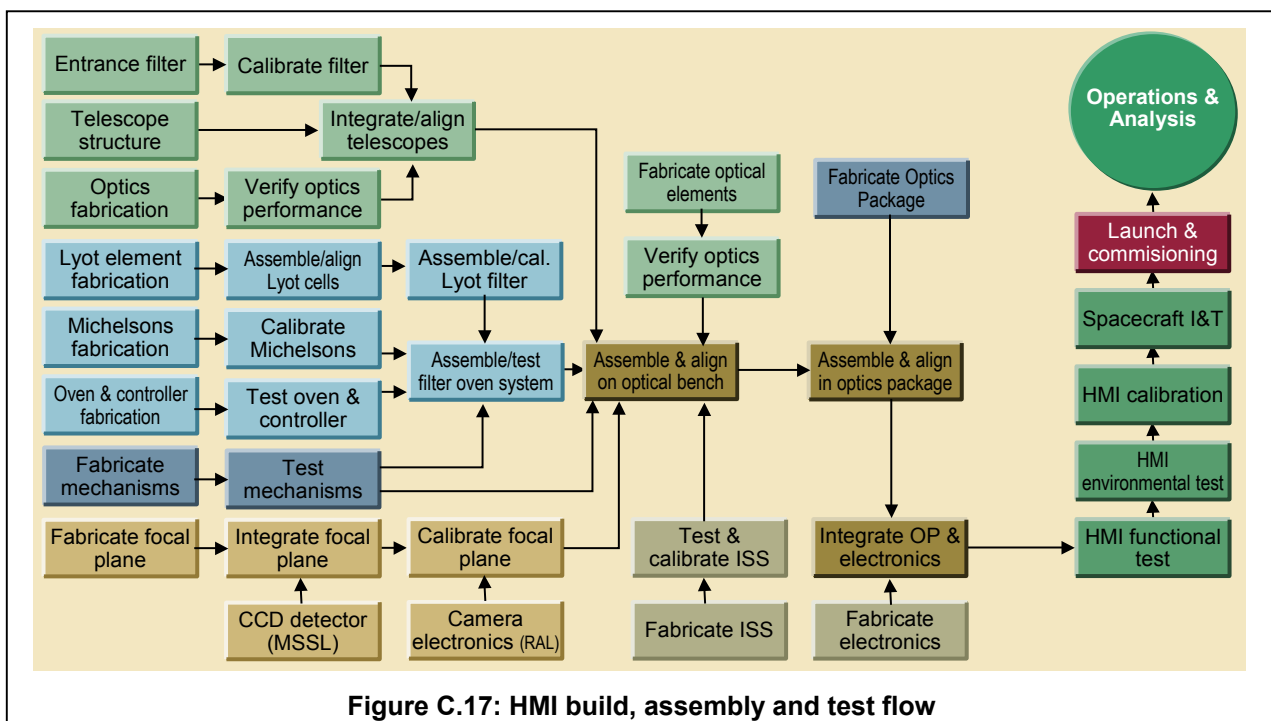
early as possible in order to undergo calibration and sunlight performance testing. The flight optics will be assembled in test fixtures on an optical table to verify their specifications and performance. The Lyot filter and Michelson interferometers will be characterized in the LMSAL filter lab using both tunable lasers and sunlight. Additional tests of the Michelsons will be performed in vacuum to measure their uniformity and verify their response to thermal transients.

The characterized optics and filters are assembled on an alignment fixture in a clean room. The combined optics and filter system performance will be carefully measured before transferring the subsystems to the flight optics structure. Final tests will be performed with sunlight, both in and out of vacuum. A brassboard camera can be used for much of the characterization testing.

The HMI fabrication, assembly, and test flow shown in **Figure C.17,** allows parallel development of the subsystems and efficient integration of the instrument. LMSAL will develop the electronics, internal mechanisms, optics and filters, and structures. RAL and MSSL will develop the CCDs and camera

electronics.

The telescope optics and entrance filter are assembled and calibrated as a subsystem prior to integration with the other optics. The Lyot filter and Michelson inteferometers are assembled and calibrated before installation in the filter oven along with the filter tuning mechanisms. The calibration/focus and polarization selector mechanisms, shutters, ISS and cameras are individually assembled and tested. All these subsystem are then integrated on an alignment fixture for calibration. All units are then transferred to the flight optics package for final testing and calibration.

The HMI electronics are developed and tested with interface simulators and brassboards prior to integration with the telescope to become the HMI instrument. The entire instrument undergoes functional and performance testing prior to the start of the formal acceptance program.

The HMI verification matrix is in **Table C.6.**

C.2.2.14 Relationship with the AIA

If both this HMI proposal and the Lockheed Martin proposal for the Atmospheric Imaging Assembly (AIA) are selected, savings will be achieved in mass, power, and developmental costs. HMI and AIA use the same CCD and CCD header designs, identical (except for the number of data channels) camera electronic designs, similar mechanisms, and the same digital and power electronic systems. The two instruments share very similar flight software and image stabilization systems. Combining HMI and AIA eliminates an electronics box and saves 12.4 kg and 21 W.

Table C.6 HMI Verification Matrix	Long Form Functional (CPT)	Short Form Functional (LPT)	EMI/EMC/Magmetics	Thermal Balance	Thermal Vacuum	Mass, Center of Gravity	Structural Loads (Quasistatic)	Modal Survey	Sine & Random Vibration	Mechanical Shock	Life Testing (Mechanical)	Pressure Profile (Launch)
FM HMI	T	T	T	T	T							
FM Electronics Box	T	T				T	T	T	T	T		A
FM Optics Package						T	T	T	T	T	T	
Telescope		T										A
Mechanisms		T							T		T	
Filter Oven System		T		T	T							
Lyot Filter		T			T							
Michelsons		T			T							
CCD Cameras		T										
Structural Thermal Model					T		T	T	T	T	T	

FM = Flight Model   T=Test; A = Analysis

C.3   Mission Operations

The goal of the HMI mission operations is to produce a uniform and continuous data set of solar Dopplergrams and magnetograms. Clean multi-day image time series are necessary for time-distance helioseismology analysis, and multi-year time series are essential for solar cycle studies. Our experience with MDI has demonstrated that even subtle changes in the observing program can influence the helioseismology analysis. Except for calibration support, we plan to operate a single observing sequence for the life of the HMI instrument in order to achieve the cleanest possible data set and a minimum level of operator support.

C.3.1   HMI Operations Support

The HMI operations are divided into three phases: launch and initial checkout, nominal operations, and coordinated spacecraft activities. During the first month after launch, the HMI instrument will be run through a pre-planned sequence of commissioning and calibration activities. The goal is to verify the correct operation of all the HMI subsystems and to tune any instrument parameters necessary to achieve optimal performance. An extensive set of calibrations will be performed to crosscheck the on-orbit HMI characteristics against the ground calibration and to optimize the long-term on-orbit calibration sequences. A series of observing sequences will be tested to determine the most efficient observing program, both in terms of the resulting science data products and instrument resources. We expect that the coordinated spacecraft activities will be rehearsed. During launch and checkout, HMI personnel will be located at the SDO Mission Operations Center (MOC) with support from the HMI Science Operations Capability (SOC) at Stanford University.

Nominal operations begin at the completion of the commissioning activities, with a single observing program similar to that described in section C.2.1. All observations require the spacecraft to maintain nominal Sun center pointing with the spacecraft roll adjusted to keep the projection of the solar rotation axis aligned to the HMI coordinate frame (similar to the SOHO spacecraft roll steering law). A complete observable cycle will have a 90 second period, and both cameras will generate a full image every 4.1 seconds. These images will be compressed to 6.1 bits/pixels using lossless compression algorithms resulting in a 50 Mb/s downlink. This sequence is only interrupted for occasional calibration and spacecraft activities, and will continue to run through the periodic SDO eclipses. The on-orbit calibration support will be very similar to that implemented with the MDI instrument. A daily sequence of images will be taken in HMI "calibration mode" to monitor instrument transmission and CCD performance. This sequence will run for one to two minutes, and will be scheduled as part of the nominal observing sequence. Approximately every four weeks, a longer performance monitoring sequence will be run to measure the instrument focus, filter and polarization characteristics. This sequence will run for one to two hours, and will likely be initiated through ground command.

The coordinated spacecraft activities envisioned are station keeping and momentum management (SK/MM) activities, and spacecraft off-point and roll maneuvers. During SK/MM activities, the HMI ISS loop will be opened to minimize the large excursions of the active mirror. The HMI ISS commands could be included in the overall SK/MM script as was done for MDI during SOHO maneuvers. The spacecraft off-point and roll maneuvers are similar to those performed by the SOHO spacecraft. These are desired at six-month intervals, near the eclipse season in order to minimize interruptions during the non-eclipse periods. The off-point is used to determine the instrument flat-field, and requires 5 minute dwells at 15 to 20 off-point positions on the solar disk. It is expected that other SDO instruments will also require spacecraft off-

points. The roll maneuver is essential to determining the solar shape, and a similar activity has been performed with MDI to make solar oblateness measurements. The spacecraft rolls allow the instrumental and solar components of the observed shape to be separated, and requires a 360º roll with 15 minute dwells at 12 to 16 evenly spaced roll angles. Depending on spacecraft performance, the off-point activity is likely to take 2 to 3 hours, and the roll activity 6 to 8 hours. The HMI observing sequence for both activities would be similar to the nominal observing sequence and could be initiated as part of a spacecraft script.

C.3.1.1 Science Operations Capability

The HMI SOC will be located at Stanford University and will be responsible for science planning and operations, instrument health and safety monitoring, and data receipt and tracking. Training materials and operations scripts will be developed in coordination with the flight operations team. These activities will be similar to those performed by the Stanford group for the MDI operation and data recovery.

After commissioning is completed, HMI operations will primarily consist of instrument health monitoring and scheduling calibration and coordinated spacecraft activities. Instrument command timelines will be generated as required (a few times per week), and sent to the MOC for upload at the next scheduled command window. The HMI health monitoring will consist of automated processing of HMI housekeeping and summary science data with alerts generated when out of nominal conditions are identified. The summary health status will be reviewed daily, and long-term instrument trends will be monitored for anomalies. The MOC support described in the AO is sufficient to meet all HMI operational requirements.

C.3.2 Data Collection, Analysis, and Archiving

The HMI SOC will manage the essentially continuous stream of data from the instrument at the nominal rate of 50 Mb/s for the duration of the mission. The data will be converted to standard formats, calibrated to physical observables, and key higher level scientific products will be produced. The SOC will capture the instrument from the SDO MOC. It will support any mission operations as required, provide key forecast and planning information, manage the internal data flow necessary to support both pipeline analysis and research, provide high-quality and easily usable data to the scientific community, and provide a safe long-term archive for the key data products.

The observing and analysis procedures for HMI do not differ fundamentally from those we have previously developed for MDI. The principal differences are: the average data rate for HMI is 500 times higher; the processing of filtergrams to observables is performed on the ground rather than onboard, allowing improved but more complex calibration procedures; HMI provides a second channel of filtergrams describing the components of the vector magnetic field, filling factor, and thermodynamic state; and Level-2 and Level-3 science data processing modules will be in place in the processing pipeline from the beginning of the mission.

We believe that the data processing and management approach that has evolved to serve MDI is a good solution to meet the needs of HMI without fundamental redesign. This conclusion is based on conservative estimates for increases in processing power and data handling technology over the next few years.

HMI is committed to an open data policy. As with MDI, HMI data will be available to the science community in each level of reduction as soon as it is available at the HMI SOC. The current best calibration parameters and soft-

ware will also be freely available. HMI will coordinate with the other SDO investigations in Phase-A to determine appropriate formats for data exchange, catalog exchange, and archive locations. We will suggest that the HMI SOC be the NASA designated mission archive for HMI data for the duration of the mission. At the conclusion of the mission the raw, reduced, and calibrated data will be deposited in appropriate NASA specified data archive.

A number of HMI data products will be of immediate value for space-weather analysis. These products will be computed from the best available data set in near real time for rapid delivery to users. The particular set will be determined in Phase-D but will certainly include full-disk magnetograms, continuum images, and farside activity images.

C.3.2.1 Observing the Archive and Processing Pipelines

A key concept in the SDO mission design is that the whole Sun will be observed all the time and events will be studied by "observing the archive". HMI supports this concept. Apart from calibration activities, HMI is designed to operate in a fixed observing mode throughout the mission, with no special instrument configurations or observing campaigns.

In addition to studies made from the archive data, many of the HMI science objectives require continuous streams of data at a higher level of processing. **Foldout.1.L** is a schematic flow diagram of this processing pipeline. The HMI SOC will provide the software and hardware infrastructure for the pipeline processing and Co-Investigators will provide software modules to generate the higher-level products.

Comparison of and combination of data from HMI and other instruments on SDO and elsewhere is vital to the goal of characterizing and understanding the solar and heliospheric complex. We expect the Virtual Solar Observatory

(VSO) to provide the framework and tools for data mining and correlative analysis. We are taking an active role in the design and development of the VSO, and we will build the HMI archive to fully interoperate with VSO and related data archives at Stanford and LMSAL. If the LMSAL AIA is also selected, we plan to integrate the data archives and data processing and distribution functions. This will result in significant cost saving, and in seamless integration of the data access tools provided to the community via the VSO.

C.3.2.2 Science Data Processing

The basic data processing flow required for HMI is data-driven, so it can be summarized as a set of sequential steps. At the first level is data input from the MOC, including sorting and depacketizing with the ability to request data from the MOC to fill in gaps. The resulting ordered raw telemetry will be permanently archived within 30 days. We expect to maintain most recent 30 days of raw data online.

Raw data reconstruction involves decompression and reconstruction into the individual filtergrams, with tags for time and instrument configuration information. These constitute the Level 0 data and will be permanently archived. Since these data correspond simply to the raw data, but are easier to use by the next level of processing, we plan to keep them online cache (nominally 3 months).

The Level 0 data are calibrated from suitable combinations of filtergrams to line parameters: continuum intensity and equivalent line width, Doppler shifts and Stokes I, Q, U, and V components. These line parameters can in turn be interpreted by suitable inversions as physical observables such as the thermodynamic state variables, line-of-sight velocity, and magnetic field strength and orientation. Images of the line parameters and/or the derived physical observables constitute the Level 1 data.

Since there is a substantial difference in complexity between the production of line parameters and some physical calibrations, and a significant difference in the degree to which certain line parameters can be used as suitable proxies for the physical observables, the decision as to which observables are to be produced routinely and archived needs to be made on a case-by-case basis. Certainly the Doppler shift data will be fully archived, as they constitute the data for most helioseismic analysis. Magnetograph-method line-of-sight field and continuum intensity will be produced at full resolution but not all of these will necessarily be archived; lower-resolution Level 2 products may be archived instead, as appropriate for the demand. We expect that vector magnetic field data will be routinely produced at full cadence and resolution only around active regions, involving only a few percent of the available data. Line depth (equivalent width) will probably not be produced at all as a regular data product. All Level 1 observables will be available on demand during the mission by processing the Level 0 data.

A pipeline analysis of the Level 1 data will produce Level 2 and Level 3 analysis data products. Level 2 data products are the results of reorganization of the Level 1 data, such as sampling, filtering, map projections, transposition, and transforms. Examples of such products that will be regularly produced and archived include temporal averages (~10 min) of derotated line-of-sight magnetograms from the magnetograph method, and full-cadence spatial averages (~4 arc-sec resolution) of the Dopplergrams. If the Level-1 data are not archived, documentation of the algorithms, of the actual code, and of the calibration data used to produce them from the Level 0 data will accompany the higher-level data products as ancillary information. Level 3 data represent the results of scientific model analysis, such as helioseismic mode fits, mode inversions, magnetic and velocity field reconstruction, and feature identification. The exact set of analysis products is to be determined in Phase D. It will include results of global-mode helioseismic analysis of the Doppler data up to medium degree, and local-area helioseismic analysis performed over regular grids, including ring-diagram and time-distance analysis and acoustic holographic imaging. It will also include such derived Level 3 information as magnetic field configurations and feature identifications.

Table C.7 shows the various levels of data products with estimates of the volumes processed, cached, and permanently archived. Whether data at any level are stored compressed or uncompressed will depend on the relative costs of storage and processing. For purposes of estimating the requirements we assume only a minimal compression factor, achievable for example by disk cropping. The cache period for the Level 1 products represents an estimated average for selected products held online for the duration of the mission

Level	Description	Examples	Rate [GB/day]	Rate [TB/yr]	Cache [day]	Archived [%]
Raw	Telemetry	-	600	200	30	100
0	Filtergrams	-	1000	400	100	100
1	Observables	V_{LOS}, B_{LOS}, I_c, EW, Stokes Parameters	400	160	600	30
2	Reorganized data	Spatial/temporal Samples, Averages; Synoptic maps	10	3	3000	100
3	Inferences	Global modes, Analysis maps, Farside images, Coronal fields	<1	<1	2000	100
Table C.7 – HMI Data Archive						

and others for only a minimal period.

If the vector magnetic field is removed from the HMI "suite" the data volume of raw data will be reduced to half but the volume of higher-level products will be essentially unchanged.

C.3.2.3   System Architecture

Based on experience with MDI processing of similar data, the system hardware configuration is currently planned as a processing farm of 100 dual-CPU Intel servers with standard 72 GB disks and Linear Tape Open (LTO) and/or high density DVD technology for off-line and near-line storage. The required combination of online and near-line cache storage is about 400 TB, and the required amount of permanent offline storage is around 450 TB per year of operation. The particular hardware architecture for the processors and data archive media will be determined two years before launch. The only constraint is the use of a Unix-family operating system to allow re-use of much of the MDI code.

The software architecture will be the basic architecture of the MDI system. Particular changes will be made to handle the HMI telemetry stream and required data product generation. A new simulation subsystem will be built to generate the telemetry formats and rates expected from HMI. There will be provisions for inserting known data so that data validation at each processing level can be performed.

The current MDI components of data validation, pipeline execution, standard data product generation, parallel virtual machine, data storage management, database server, data catalog, Oracle DBMS, media archive server, quality reporter, job management, SOAP data query URL, and extensive data export methods will be retained with modifications for the HMI demands. As a result, large-scale system prototyping can begin immediately following the initial system engineering studies.

Changes do need to be made to data formats, and to remove hardware specific dependencies from some components.

C.3.2.4   Data Organization

The MDI data management approach was built around the concept of using a widely-accepted standard data format (FITS) for most data products, and organizing the data archive by collections of such files. While this approach proved sound from the viewpoint of handling what was at the time a comparatively large data archive and providing useful data to the community rapidly with comparatively little user effort and required support, it imposed constraints that proved a serious inconvenience in the effort to provide the best calibrated data. These arose primarily from the necessity of binding the ancillary per record data to the image data, so that any change in a single calibration value, for example, required re-archiving an entire set (hour or day) of images.

An alternative approach is to archive the data in a private format suitable for quick access and manipulation, and to provide the necessary tools for users to be able to interpret the data and process them on the fly. We intend to follow a compromise path for HMI. We will produce higher level data products, but keep the data in very simple private formats, and provide basic tools to convert them to a standard format as required. An example is detachment of the header and data records of FITS files in the archive, to be combined at the point of access. This will allow us to maintain the powerful and efficient MDI data system for managing the bulk data via the database of image sets and a mixed-media archive, while also benefiting from the ability to use a complete online archive of ancillary data at the record level.

REFERENCES FOR SECTION C.2

1. Scherrer, P.H., et al., 1995. *The Solar Oscillations Investigation - Michelson Doppler Imager.* Solar Physics, **162**: p. 129.

2. Corliss, C. and J. Sugar, 1981. *Energy Levels of Nickel, Ni I through Ni XXVIII.* J. Phys. Chem. Ref. Data, **10**(1): p. 197.

3. Rees, D. in *Numerical Radiative Transfer*. 1987.

4. Jefferies, J., B. Lites, and A. Skumanich, 1989. *Transfer of Line Radiation in a Magnetic Field.* Astrophysical Journal, **343**: p. 920.

5. Landi Degl'Innocenti, E., *Magnetic Field Measurements*, in *Solar Observations: Techniques and Interpretation*, F. Sánchez, M. Collados, and M. Vázquez, Editors. 1992. p. 71.

6. Hagyard, M.J. and J.I. Kineke, 1995. *Improved Method for Calibrating Filter Vector Magnetographs.* Solar Physics, **158**: p. 11.

7. Sakurai, T., et al., 1995. *Solar Flare Telescope at Mitaka.* PASJ, **47**: p. 81.

8. Graham, J.D., et al., 2002. *Inference of Solar Magnetic Field Parameters from Data with Limited Wavelength Sampling.* Solar Physics: p. in press.

9. López Ariste, A. and M. Semel, 1999. *DIAGONAL: A numerical solution of the Stokes transfer equation.* A & AS, **139**: p. 417.

10. Akin, D., R. Horber, and J. Wolfson. *Three High Duty Cycle, Space-Qualified Mechanisms*. in *27th Aerospace Mechanisms Symposium*. 1993. Moffett Field, CA: NASA.

11. Kuhn, J.R., H. Lin, and D. Loranz, 1991. *Gain Calibrating Nonuniform Image-array Data Using Only the Image Data.* Astronomical Society of the Pacific Publications, **103**: p. 1097.